Volume doubling time and radiomic features predict tumor behavior of screen-detected lung cancers

Jaileene Pérez-Morales[a], Hong Lu[b], Wei Mu[b], Ilke Tunali[b,c], Tugce Kutuk[d], Steven A. Eschrich[e], Yoganand Balagurunathan[e], Robert J. Gillies[b] and Matthew B. Schabath[a,f,*]

[a]*Department of Cancer Epidemiology, H. Lee Moffitt Cancer Center and Research Institute, Tampa, FL, USA*
[b]*Department of Cancer Physiology, H. Lee Moffitt Cancer Center and Research Institute, Tampa, FL, USA*
[c]*Institute of Biomedical Engineering, Bogazici University, Istanbul, Turkey*
[d]*Department of Radiation Oncology, H. Lee Moffitt Cancer Center and Research Institute, Tampa, FL, USA*
[e]*Department of Bioinformatics and Biostatistics, H. Lee Moffitt Cancer Center and Research Institute, Tampa, FL, USA*
[f]*Department of Thoracic Oncology, H. Lee Moffitt Cancer Center and Research Institute, Tampa, FL, USA*

Abstract.

BACKGROUND: Image-based biomarkers could have translational implications by characterizing tumor behavior of lung cancers diagnosed during lung cancer screening. In this study, peritumoral and intratumoral radiomics and volume doubling time (VDT) were used to identify high-risk subsets of lung patients diagnosed in lung cancer screening that are associated with poor survival outcomes.

METHODS: Data and images were acquired from the National Lung Screening Trial. VDT was calculated between two consequent screening intervals approximately 1 year apart; peritumoral and intratumoral radiomics were extracted from the baseline screen. Overall survival (OS) was the main endpoint. Classification and Regression Tree analyses identified the most predictive covariates to classify patient outcomes.

RESULTS: Decision tree analysis stratified patients into three risk-groups (low, intermediate, and high) based on VDT and one radiomic feature (compactness). High-risk patients had extremely poor survival outcomes (hazard ratio [HR] = 8.15; 25% 5-year OS) versus low-risk patients (HR = 1.00; 83.3% 5-year OS). Among early-stage lung cancers, high-risk patients had poor survival outcomes (HR = 9.07; 44.4% 5-year OS) versus the low-risk group (HR = 1.00; 90.9% 5-year OS). For VDT, the decision tree analysis identified a novel cut-point of 279 days and using this cut-point VDT alone discriminated between aggressive (HR = 4.18; 45% 5-year OS) versus indolent/low-risk cancers (HR = 1.00; 82.8% 5-year OS).

CONCLUSION: We utilized peritumoral and intratumoral radiomic features and VDT to generate a model that identify a high-risk group of screen-detected lung cancers associated with poor survival outcomes. These vulnerable subset of screen-detected lung cancers may be candidates for more aggressive surveillance/follow-up and treatment, such as adjuvant therapy.

Keywords: Radiomics, LDCT, NLST, CART, early detection, VDT

*Corresponding author: Matthew B. Schabath, H. Lee Moffitt Cancer Center and Research Institute, 12902 Magnolia Drive MRC-CANCONT, Tampa, FL 33612, USA. Fax: +1 813 745-4150; E-mail: matthew.schabath@moffitt.org.

1. Introduction

Four randomized clinical trials demonstrated that screening and early detection of lung cancer by low-dose helical computed tomography (LDCT) reduces

overall and lung cancer-specific mortality [1,2,6,11,33]. However, despite the benefits of early detection, cancer screening can result in overdiagnosis which is the detection of asymptomatic cancers that are non-growing or slow-growing and unlikely fatal if left untreated [10]. Overdiagnosis of pulmonary nodules can result in unnecessary diagnostic procedures that are often invasive, associated with increased costs, and associated with added stress for patients and their families [52]. In the US National Lung Screening Trial (NLST), 10 to 27% lung cancers were overdiagnosed in the LDCT arm of the study [27,34,41–43]. As such, biomarkers that can discriminate between the variability in growth rates and lethal potential [42] of lung cancers diagnosed in lung cancer screening would have important clinical translational implications.

Radiomics is the conversion of medical images into structured, mineable data that can subsequently be utilized for statistical analysis and modeling [9,12,13,17, 25,28,29,44]. Radiomic features have shown to provide rapid and accurate noninvasive biomarkers for lung cancer risk prediction, diagnostics, prognosis, treatment response monitoring, and tumor biology [15,45,47]. Radiomics have many advantages over tissue-based biomarkers as they are generated from standard-of-care imaging and they reflect the pathophysiology of the entire imaged tumor or region-of-interest (e.g., screen-detected nodule) and not just the portion of the tumor that was assayed in the case for tissue-based biomarkers.

Volume doubling time (VDT) of a pulmonary nodule, defined as the number of days in which the nodule doubles in volume, is a clinically relevant metric in lung cancer screening. VDT has clinical utility in discriminating between nodules that are infectious/inflammatory, malignant, and benign [30,46,51]. Generally, nodules that are of an infectious or inflammatory pathophysiology have a VDT of less than 20 days, a VDT of less than 400 days (and greater than 20 days) represents a high likelihood of malignancy, and a VDT above 500 days is likely a benign nodule [23,24]. To date, there have been few studies analyzing VDT, a delta-radiomic, as a potential biomarker to evaluate lethal potential of lung cancers diagnosed in lung cancer screening. Thus, using publicly available data and LDCT images from the NLST, we generated radiomic features to determine if we can discriminate between indolent, slow, and aggressive incidentally diagnosed lung cancers. Radiomic features describing size, shape, volume, growth rate (i.e., VDT), and textural characteristics were calculated from the intratumoral region (area

within the tumor) and from the peritumoral region (area surrounding the tumor parenchyma). The overarching goal of this study was to utilize radiomics biomarkers to generate parsimonious models to predict lung cancer outcomes in the lung cancer screening setting.

2. Materials and methods

2.1. NLST study population

Deidentified LDCT images and data were obtained from the National Cancer Institute (NCI) Cancer Data Access System (CDAS) [14]. The NLST study design and main findings have been described previously [1,2]. NLST eligibility criteria included current and former smokers aged 55–74 years with a minimum 30 pack-years smoking history and former smokers had to have quit within the past 15 years.

The present study used a subset of lung cancers diagnosed in the LDCT-arm of the NLST and has been described elsewhere [38]. Briefly, we identified 314 screen-detected, incident lung cancer patients who were not diagnosed with lung cancer at baseline screening (T0) but were subsequently diagnosed with lung cancer either at the first follow-up screening (T1) or second follow-up screening (T2). However, participants were excluded due to several reasons: unavailable complete volumetric images sets, nodules at baseline that could not be identified, and nodules where it was difficult to contour the tumor. Lung cancer patients who had multiple nodules at time of their diagnosis were excluded ($N = 20$) since we are unable to verify which nodule(s) were cancer.

The final analytical cohort included 94 participants who had a negative or positive baseline LDCT screening. Based on NLST criteria, positive screens were defined as abnormalities on baseline screens or at follow-up screens that were new, stable or evolved that resulted as one or more non-calcified masses measuring $\geqslant 4$ mm in axial diameter [38]. Negative screens were defined as having no abnormalities, minor abnormalities, or significant abnormalities not suspicious for lung cancer.

2.2. Radiomics

Nodule identification and tumor segmentation has been described in detail elsewhere [17]. Briefly, the tumor mask images (i.e., tumor delineations) were imported into in-house radiomic feature extraction toolboxes created in MATLAB® 2015b (The Mathworks
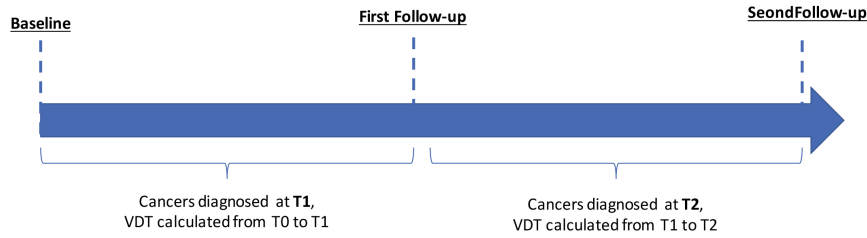
Fig. 1. Schema for identification of patients diagnosed with cancer at two different timepoints in the NLST.

Inc., Natick, Massachusetts) and C++ (https://isocpp. org). Using cubic interpolation, the images were resampled to a single voxel spacing of 1 mm × 1 mm × 1 mm to standardize spacing across all images. Hounsfield units (HU) in all images were resampled into fixed bin sizes of 25 HUs discretized from -1000 to 1000 HU.

Using standardized radiomic algorithms from the Image Biomarker Standardization Initiative (IBSI) v5 [56], a total of 264 radiomic features were extracted from the semi-automatically segmented intratumoral region ($n = 155$) and from the peritumoral region ($n = 109$) 3 mm outside of the tumor boundary. The peritumoral regions were generated as an extension of the tumor segmentations using morphological image processing operations as previously described [48]. Peritumoral regions were bounded by a lung parenchyma mask to exclude the region of interest (ROI) outside of the lung parenchyma. Shape- and size-based peritumoral features were excluded as they explicitly describe and correlate with the intratumoral ROI. The 65 most stable and reproducible intratumoral and peritumoral radiomic features that were previously found by our group [48] were utilized for analysis.

Volume doubling time was calculated for the screening interval from T0 to T1 and for the screening interval from T1 to T2 (Fig. 1). Below is the equation for VDT where Ti is the time interval between two LDCT imaging studies, V_i is the volume of the nodule in the second LDCT image, and V_0 is the volume of nodule in the first LDCT image:

$$VDT = \frac{\ln 2x T_i}{\ln \left(\frac{V_i}{V_0} \right)}$$

2.3. Radiogenomics analysis

A previously described dataset [39] of surgically resected adenocarcinoma lung cancers who had pre-surgery CTs and gene expression data was used to identify potential biological underpinnings of the most informative radiomic features identified in our analyses. The gene probesets were filtered and determined as sig-nificant using the following criteria based on a Student's t test $p < 0.001$ and mean log fold-change between high and low prognostic radiomic feature of lfc > log2 (1.4 FC). The significant probesets from the analyses were intersected yielding a final list of probesets significantly associated with the most informative radiomic features. ANOVA and Tukey pairwise mean comparison was performed to analyzed gene expression across the risk groups.

2.4. Statistical analysis

Statistical analyses were performed using Stata/MP 14.2 (StataCorp LP, College Station TX), R Project for Statistical Computing (version 3.5.2), and R Studio (version 1.1.463).

Overall survival (OS) and progression-free survival (PFS) were the main endpoints and were assessed from date of lung cancer diagnosis to the date of an event or last follow up. For OS, an event was defined as death and for PFS an event was established as death or progression of cancer. All survival data were right censored at 5-years.

To generate a parsimonious model, the 65 stable radiomic features and VDT were subjected to Classification and Regression Tree (CART) analysis, adapted for survival analysis, to stratify patients into risk groups. The risk groups were analyzed by Cox regression models, Kaplan-Meier survival curves, and log-rank tests. The most informative radiomic features identified in the CART analysis were internally cross-validated using R package "rms" [16]. The Harrell's concordance index (C-index) was used to evaluate the performance of the multivariable Cox regression models. Backward logistic regression model was used to identify radiomics features significantly associated with VDT dichotomized.

3. Results

3.1. Patient characteristics

The demographics of the lung cancer patients are provided in Table 1. Mean age of enrollment into the

Table 1
Patient characteristics

Characteristics	All patients (N = 94)
Age, mean(sd)	64.3 (5.4)
Sex	
Female	39 (41.5%)
Male	55 (58.5%)
Smoking status	
Former	39 (41.5%)
Current	55 (58.5%)
Pack-years smoked mean (sd)	63.4 (23.9)
Self-reported COPD	
No	81 (86.2%)
Yes	13 (13.8%)
Family history of lung cancer	
No	72 (76.6%)
Yes	22 (23.4%)
Histology	
Adenocarcinoma-BAC	52 (55.3%)
Small cell	3 (3.2%)
Squamous	18 (19.2%)
Other NOS	21 (22.3%)
Stage	
I and II	76 (80.8%)
III and IV	18 (19.2%)
Treatment	
Surgical	74 (78.7%)
Chemotherapy/other	6 (6.4%)
Radiation	14 (14.9%)
Baseline screening (T0)	
Positive (T0+)	40 (42.6%)
Negative (T0−)	54 (57.4%)

Abbreviations: sd = standard deviation; FH = family history; Pack-years = packs smoked/day x years smoked; COPD = chronic obstructive pulmonary disease; NOS = not otherwise specified; [1]BAC and adenocarcinoma were combined into one group.

NLST was 64.3 years, 58.5% participants were male, 58.5% were current smokers, 55.3% were diagnosed with adenocarcinoma, and 80.8% had an early-stage lung cancer (stage I or II).

3.2. Screening interval from T0 to T1

Radiomics were calculated from LDCT images at T0 and VDT was calculated from T0 to T1 as seen in Fig. 2A. The mean number of days between T0 and T1 was 369 days (range: 282 to 620 days). VDT was not significantly correlated to intratumoral or peritumoral features. VDT and the 65 radiomic features that we identified as stable and reproducible were included as inputs into CART analysis and subsequent decision tree revealed four risk groups as terminal nodes: low-risk, intermediate-risk, high-risk, and very-high-risk (Fig. 2B). The decision tree structure included VDT and two radiomic features (intratumoral feature compactness and peritumoral feature average co-occurrence).

There are differences in VDT across the four risk-groups. The very-high risk group has a lower VDT (median VDT: 108.56) between T0 to T1 when compared to the high, intermediate, and low risk group (median VDT: 114.6, 143.2, and 499.2, respectively). From T0 to T1, Kruskal-Wallis test revealed that there is a statistically significant difference in VDT between the four risk groups ($P = 0.0001$). Pairwise analyses revealed, that when compared to the low-risk group, VDT was statistically significant different for the intermediate-risk ($P < 0.0001$), high-risk group ($P < 0.0001$), and very-high risk group ($P < 0.0001$) as presented in Fig. 2B. CART analysis identified a novel VDT threshold (i.e., cutpoint) of 234 days which discriminated between high-risk lung cancers (HR = 3.49; 40% 5-year OS) versus low-risk cancers (HR = 1.00; 80.8% 5-year OS) (Fig. 2C). Similar results were observed for PFS (Supplemental Fig. 1A). The very-high-risk group (Fig. 2D) was associated with extremely poor OS (HR = 11.71; 42.9% 2-year OS and 21.4 % 5-year OS, log-rank $P < 0.0001$) versus the high (HR = 5.08; 82.4% 2-year OS and 22.9% 5-year OS), intermediate (HR = 1.61; 93.3% 2-year OS and 72.7% 5-year OS) and low-risk group (HR = 1.00; 89.5% 2-year OS and 82.1% 5-year OS). Similar findings were observed for PFS (Supplemental Fig. 2A). Among early-stage patients, the very-high-risk group was associated with extremely poor survival (HR = 14.84; 33.3% 2-year and 33.3% 5-year OS, log-rank $P < 0.001$) versus the low-risk group (HR = 1.00; 95.2% 2 year and 90.4% 5-year OS) (Fig. 2E). Among late-stage patients, there was no significant association with OS (Fig. 2F). Similar results were found for PFS (Supplemental Fig. 2B and C).

There were no statistically significant differences between the four risk groups by age, smoking status, number of pack-years smoked, baseline screening, and family history of lung cancer (Table 2). However, there were statistically significant differences across the risk groups for sex ($P = 0.02$), self-reported COPD ($P = 0.003$), histology ($P = 0.007$), treatment ($P = 0.038$), and stage of disease ($P = 0.042$). In terms of lung cancer stage, 64.3% of the patients in the very-high-risk group had lung cancer early-stage vs. 87.5% in the low-risk group ($P = 0.042$). As such, multivariable Cox regression models were used to adjust for potential confounding factors including sex, treatment, self-reported COPD, and stage. The very-high-risk group was associated with an elevated hazard ratio (OS: HR = 10.90; 95% Confidence Interval: [3.98, 29.85] and PFS: HR = 4.72; 95% Confidence Interval: [1.85, 12.07]) when compared to high, intermediate, and low-risk groups
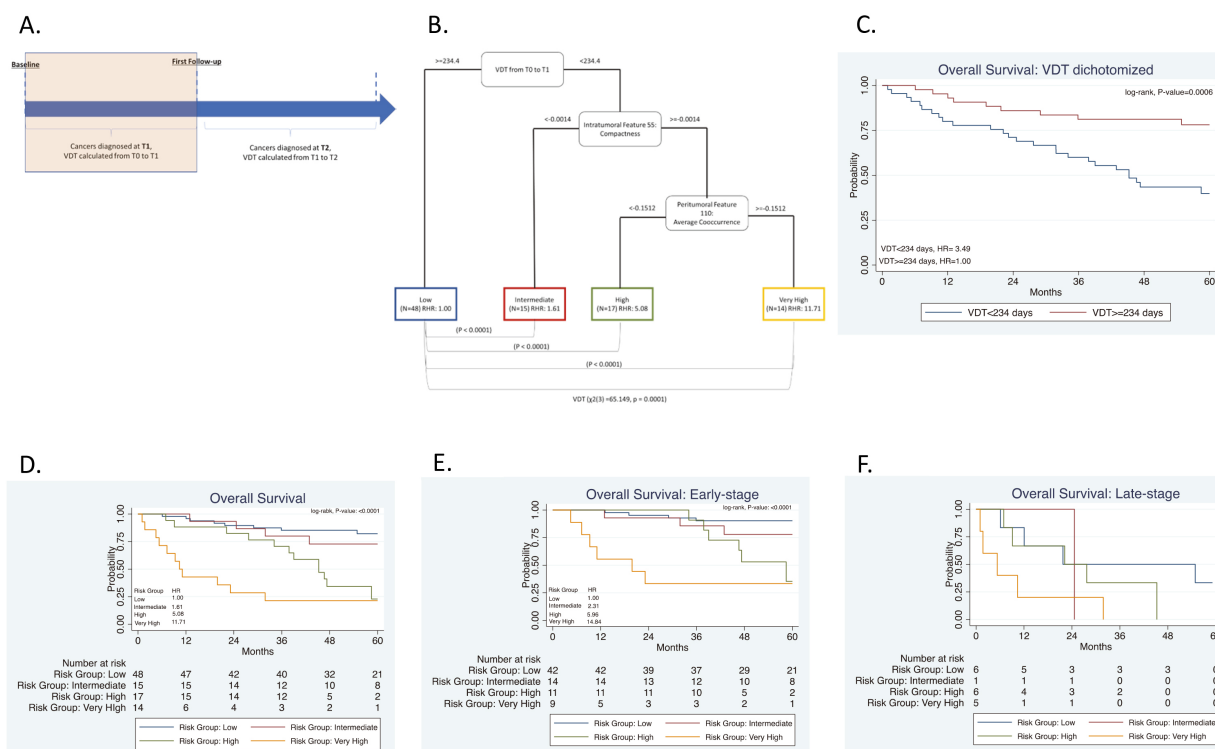
Fig. 2. Risk-groups associated with overall survival for all patients and among early-stage patients diagnosed in the screening interval T0 to T1. (A) Schema identifying patients diagnosed in the screening interval T0 to T1. (B) The tree structure from the classification and regression tree (CART) analysis identified four risk groups based on two radiomics features and VDT. VDT was statistically significant different between very-high, high, and intermediate when compared to low-risk group. (C) Overall survival for VDT dichotomized by 234 days. Overall survival for the risk patient risk groups among all patients (D) and for early-stage (E), and for late-stage patients (F).

(Table 3 and Supplemental Table 1) with a C-index of 0.85. The multivariable model using 10-fold cross validation achieved high prediction performance (C-index = 0.81). Among early-stage patients, the very-high-risk group was associated with an elevated hazard ratio (OS: HR = 21.63; 95% Confidence Interval: [3.70, 123.60] and PFS: HR = 5.92; 95% Confidence Interval: [1.81, 12.07]) when compared to high, intermediate and low-risk groups (Table 3 and Supplemental Table 1) with a C-index of 0.84.

3.3. Screening intervals from T0 to T1 and T1 to T2

For this analysis, we utilized the data from Section 3.2 above and included participants who were diagnosed with lung cancer at T2. Radiomics were calculated from T0 and VDT was calculated from T0 to T1 and between T1 to T2, as seen in Fig. 3A. The mean number of days between T1 and T2 was 370 days (range: 287 to 480 days). The same stable radiomic features were combined with VDT and subjected to CART analysis and revealed three risk groups: low-risk,

intermediate-risk, high-risk (Fig. 3B). Due to the addition of participants who were diagnosed with lung cancer at T2, a new decision tree structure was identified. The decision tree structure included one radiomic feature (intratumoral feature compactness) and VDT. There are differences in VDT across the three risk-groups. The high-risk group has a lower VDT (median VDT: 104.58) between T0 to T1 and from T1 to T2 when compared to the intermediate, and low risk group (median VDT: 132.53 and 459.23, respectively) ($P = 0.0001$). Pairwise analyses demonstrated, that when compared to the low-risk group, median VDT was statistically significant different for intermediate-risk ($P < 0.0001$) and high-risk group ($P < 0.0001$) as presented Fig. 3B. CART identified a novel VDT threshold (VDT = 279 days) that discriminated between high-risk lung cancers (HR = 4.18; 45% 5-year OS) and low-risk lung cancers (HR = 1.00; 82.8% 5-year OS) (Fig. 3C). Similar results were observed for PFS (Supplemental Fig. 1B). The high-risk group was associated with extremely poor OS (Hazard Ratio (HR) = 8.15; 56.3% 2-year OS and 25.0 % 5-year OS, log-rank $P < 0.0001$)
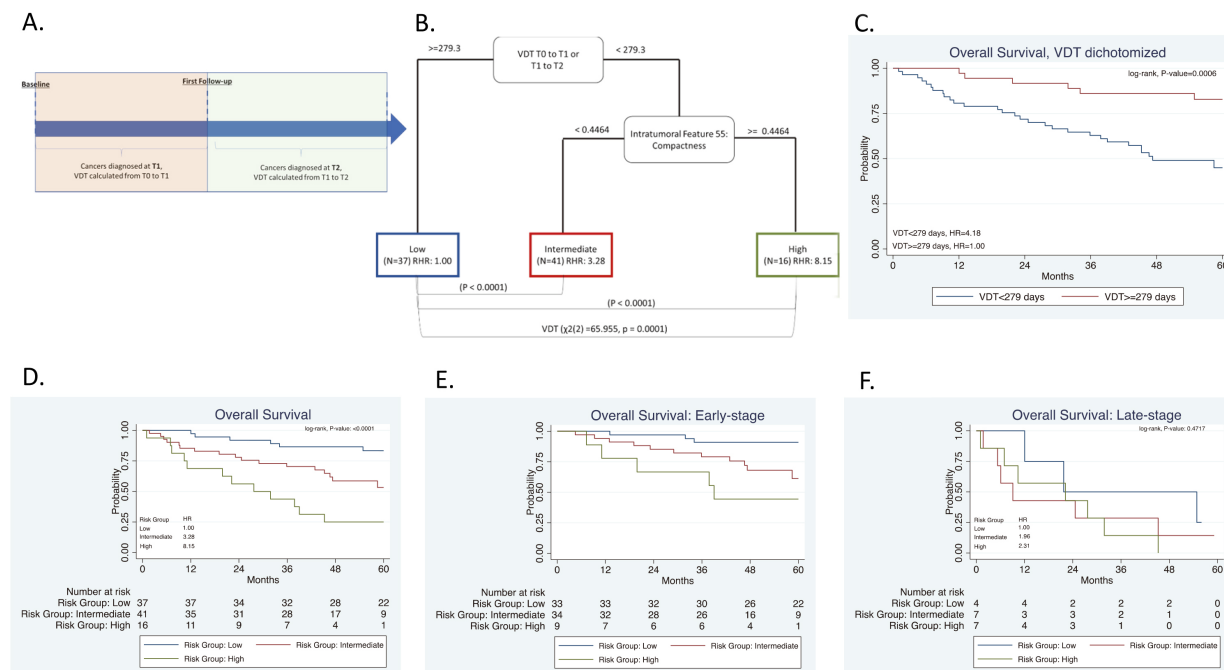
Fig. 3. Risk-groups associated with overall survival for all patients and among early-stage patients diagnosed in the screening interval T0 to T1 or T1 to T2. (A) Schema including patients diagnosed in the screening interval T1 to T2. (B) The tree structure from the classification and regression tree analysis (CART) identified three risk groups based on one radiomics feature and VDT. VDT was statistically significant different between high- and intermediate risk groups when compared to low-risk group. (C) Overall survival for VDT dichotomized by 279 days. Overall survival for the risk patient risk groups among all patients (D) and for early-stage (E), and for late-stage patients (F).

versus the intermediate (HR = 3.28; 78.0% 2-year OS and 53.3% 5-year OS), and low-risk group (HR = 1.00; 100.0% 2-year OS and 83.3% 5-year OS) (Fig. 3D). Similar findings were observed for Progression Free Survival (PFS) (Supplemental Fig. 3A). Among early-stage patients, the high-risk group was associated with a significantly decreased OS (HR = 9.07; 66.7% 2-year and 44.4% 5-year OS, log-rank $P < 0.0001$) versus the low-risk group (HR = 1.00; 96.9% 2-year and 90.9% 5-year OS) (Fig. 3E). When stratifying by late-stage patients, there was no significant association with OS (Fig. 3F). Similar results were found for PFS (Supplemental Fig. 3B and C).

There were no statistically significant differences between the three risk groups by age, smoking status, number of pack-years smoked, treatment, baseline screening, and family history of lung cancer (Table 2). However, there were statistically significant differences across the risk groups for sex ($P = 0.003$), self-reported COPD ($P = 0.003$), histology ($P =< 0.0001$), and stage of disease ($P = 0.018$). In term of lung cancer stage, 56.3% of the patients in the high-risk group had lung cancer early-stage vs. 89.2% in the low-risk group ($P = 0.018$). As such, multivariable Cox regression

models were used to adjust for potential confounding factors including sex, treatment, and stage. The high-risk group was associated with an elevated hazard ratio (OS: HR = 3.62; 95% CI: [1.12, 11.69] and PFS: HR = 2.33; 95% CI: [0.90, 6.05]) when compared to intermediate, and low-risk groups (Table 3 and Supplemental Table 1) with a C-index of 0.78 in OS. Among early-stage patients, the high-risk group was associated with an elevated hazard ratio (OS: HR = 7.82; 95% Confidence Interval: [1.44, 42.43] and PFS: HR = 3.30; 95% Confidence Interval: [0.88, 12.35]) when compared to intermediate and low-risk groups (Table 3 and Supplemental Table 1) with a C-index of 0.72 in OS.

3.4. Predicting VDT using T0 radiomics features

When dichotomizing VDT by the novel threshold of 279 days, backward logistic regression identified the intratumoral radiomic feature compactness as the most informative radiomic feature (OR: 2.54; 95% CI 0.91, 7.12]). Compactness 2, a morphological feature, is a measure of how compact the shape of the region-of-interest is relative to a sphere (most compact) [3]. Compactness 2 was ex-

Table 2
Patient characteristics by risk group

Characteristics	Screening interval from T0 to T1					Screening interval from T0 to T1 or T1 to T2			
	Low risk group (N = 48)	Intermediate risk group (N = 15)	High risk group (N = 17)	Very high risk group (N = 14)	P-value[1,2,3]	Low risk group (N = 37)	Intermediate risk group (N = 41)	High risk group (N = 16)	P-value[1,2,3]
Age, mean (sd)	62.6 (5.2)	64.4 (5.0)	65.2 (6.1)	68.3 (3.4)	0.13	63.7 (5.3)	63.8 (5.4)	66.6 (5.0)	0.93
Sex, N (%)					**0.02**				**0.0003**
Female	27 (56.3%)	4 (26.7%)	5 (29.4%)	3 (21.4%)		23 (62.2%)	10 (24.4%)	6 (37.5%)	
Male	21 (43.7%)	11 (73.3%)	12 (70.6%)	11 (78.6%)		14 (37.8%)	31 (75.6%)	10 (62.5%)	
Smoking status, N (%)					0.60				0.93
No	20 (41.7%)	8 (53.3%)	5 (29.4%)	6 (42.9%)		16 (43.2%)	17 (41.5%)	6 (37.5%)	
Yes	28 (58.3%)	7 (46.7%)	12 (70.6%)	8 (57.1%)		21 (56.8%)	24 (58.5%)	10 (62.5%)	
Pack-years, mean (sd)	60.1 (19.5)	72.4 (33.3)	66.7 (25.2)	63.9 (24.7)	0.06	62.7 (19.8)	62.8 (26.9)	66.7 (26.2)	0.16
FH of lung cancer, N (%)					0.15				0.39
No	40 (83.3%)	10 (66.7%)	14 (82.4%)	8 (57.1%)		31 (83.8%)	30 (73.2%)	11 (68.8%)	
Yes	8 (16.7%)	5 (33.3%)	3 (17.6%)	6 (42.9%)		6 (16.2%)	11 (26.8%)	5 (31.3%)	
Self-reported history of COPD, N (%)					**0.003**				**0.003**
No	45 (93.8%)	14 (93.3%)	10 (58.8%)	12 (85.7%)		36 (97.3%)	35 (85.4%)	10 (62.5%)	
Yes	3 (6.2%)	1 (6.7%)	7 (41.2%)	2 (14.3%)		1 (2.7%)	6 (14.6%)	6 (37.3%)	
Histology, N (%)					**0.007**				**< 0.0001**
Adenocarcinoma-BAC[4]	30 (62.5%)	7 (46.7%)	7 (41.2%)	8 (57.1%)		29 (78.4%)	18 (43.9%)	5 (31.3%)	
Squamous	6 (12.5%)	7 (46.7%)	2 (11.8%)	3 (21.4%)		3 (8.1%)	12 (29.3%)	3 (18.8%)	
Small cell	0 (0%)	0 (0%)	1 (5.9%)	2 (14.3%)		0 (0%)	0 (0%)	3 (18.8%)	
Other NOS	12 (25%)	1 (6.7%)	7 (41.2%)	1 (7.1%)		5 (13.5%)	11 (26.8%)	5 (31.3%)	
Treatment, N (%)					**0.038**				0.19
Surgical	42 (87.5%)	13 (86.7%)	11 (64.7%)	8 (14.3%)		33 (89.2%)	31 (75.6%)	10 (62.5%)	
Chemotherapy/other	4 (8.33%)	0 (0%)	1 (5.9%)	1 (7.1%)		2 (5.4%)	2 (4.9%)	2 (12.5%)	
Radiation therapy	2 (4.17%)	2 (13.3%)	5 (29.4%)	5 (35.7%)		2 (5.4%)	8 (19.5%)	4 (25.0%)	
Staging, N (%)					**0.04**				**0.02**
Early stage (I and II)	42 (87.5%)	14 (93.3%)	11 (64.7%)	9 (64.3%)		33 (89.2%)	34 (82.9%)	9 (56.3%)	
Late stage (III and IV)	6 (12.5%)	1 (6.7%)	6 (35.3%)	5 (35.7%)		4 (10.8%)	7 (17.1%)	7 (43.8%)	
Baseline screening, N (%)					0.11				0.12
Positive (T0+)	26 (54.2%)	5 (33.3%)	4 (23.5%)	5 (35.7%)		20 (54.1%)	16 (39.0%)	4 (25.0%)	
Negative (T0−)	22 (45.8%)	10 (66.7%)	13 (76.5%)	9 (64.3%)		17 (45.9%)	25 (61.0%)	12 (75.0%)	

Abbreviations: sd = standard deviation; FH = family history; Pack-years = packs smoked/day x years smoked; COPD = chronic obstructive pulmonary disease; NOS = not otherwise specified. [1] P-value obtained from Chi-squared for categorical variables. [2] P-value obtained from Anova for continuous variables. [3] P-value obtained from Log-rank for survival variables. [4] BAC and adenocarcinoma were combined into one group.

Table 3
Multivariable Cox proportional hazards models for overall survival

Characteristic	Screening interval from T0 to T1		Screening interval from T0 to T1 or T1 to T2	
	All patients[2] HR (95% CI)	Early-stage patients HR (95% CI)	All patients[2] HR (95% CI)	Early-stage patients HR (95% CI)
Risk group				
Low	1.00 (Reference)	1.00 (Reference)	1.00 (Reference)	1.00 (Reference)
Intermediate	1.12 (0.30, 4.13)	2.28 (0.37, 14.08)	2.38 (0.85, 6.61)	3.38 (0.85, 13.45)
High	**3.12 (1.11, 8.75)**	**9.66 (1.37, 67.99)**	**3.62 (1.12, 11.69)**	**7.82 (1.44, 42.43)**
Very high	**10.90 (3.98,29.85)**	**21.36 (3.70, 123.60)**	n/a	n/a
Sex				
Female	1.00 (Reference)	1.00 (Reference)	1.00 (Reference)	1.00 (Reference)
Male	1.61 (0.68, 3.85)	2.96 (0.55, 15.97)	1.46 (0.62, 3.43)	1.96 (0.60, 6.40)
Stage				
I and II	1.00 (Reference)	1.00 (Reference)	1.00 (Reference)	1.00 (Reference)
III and IV	**8.25 (3.42, 19.90)**	n/a	**7.03 (3.10, 15.93)**	n/a
Histology				
Adenocarcinoma-BAC[1]	1.00 (Reference)	1.00 (Reference)	1.00 (Reference)	1.00 (Reference)
Squamous	**2.84 (1.01. 7.97)**	3.05 (0.73, 12.78)	1.38 (0.55, 3.47)	1.08 (0.35, 3.35)
Small cell	1.45 (0.33, 6.42)	n/a	1.52 (0.32, 7.23)	n/a
Other NOS	0.84 (0.28, 2.53)	0.31 (0.04, 2.11)	0.66 (0.26, 1.65)	0.69 (0.19, 2.53)
Self-reported COPD				
No	1.00 (Reference)	1.00 (Reference)	1.00 (Reference)	1.00 (Reference)
Yes	2.49 (0.91, 6.81)	2.45 (0.61, 9.77)	2.10 (0.76, 5.81)	1.07 (0.29, 3.99)
Treatment				
Surgical	1.00 (Reference)	1.00 (Reference)	n/a	n/a
Chemotherapy/other	**6.58 (1.48, 29.36)**	**372.88 (12.99, 10707.83)**	n/a	n/a
Radiotherapy	**3.61 (1.43, 9.11)**	2.13 (0.53, 8.51)	n/a	n/a
Harrell's C-index	0.85	0.84	0.80	0.72

Abbreviations: COPD = chronic obstructive pulmonary disease; NOS = not otherwise specified; 1BAC and adenocarcinoma were combined into one group. Bold values represent statistically significant.

tracted from the semi-automatically segmented intratumoral region and peritumoral 3 mm outside of tumor boundary. Intratumoral Compactness 2 was identified as a stable and reproducible radiomic feature [48].

According to Aerts et al. [3] the formula is:

$$F_{morph.comp.2} = 36\pi \frac{V^2}{A^3}$$

To identify a potential prognostic threshold, compactness was included into CART to identify the most informative cutpoint associated with OS (Fig. 4A). A VDT < 279 and Compactness >= 0.60 had similar prognosis capabilities with poor outcomes (Fig. 4B).

3.5. Radiogenomics analysis

To reduce false positives in the radiogenomics analysis, we utilized a very high p-value threshold ($P < 0.0001$) to identify gene probesets associated with Compactness. From the radiogenomic analyses, MIR34A was found to be most significant gene associated ($P = 2.01E-05$) with the compactness radiomic features (Fig. 5). When Compactness was dichotomized at the median, mean VDT was higher in Compactness low vs

Compactness high (mean = 999.84 [3522.55] vs 656.60 [SD = 2345.99] ($P = 0.007$).

4. Discussion

Overdiagnosis is a serious adverse effect of cancer screening and early detection. A recent meta-analysis of randomized trials on overdiagnosis of lung cancer with LDCT [7] estimated that 49% of the LDCT screen-detected cancers may be overdiagnosed. Though the authors conclude, "there is great uncertainty about the degree of overdiagnosis in lung cancer screening due to the heterogeneity" of screening trials, there is substantial evidence [7,11,18,35,42] that overdiagnosis is a real world problem and robust biomarkers such as radiomics could have translational implications by risk stratifying screen-detected lung cancer. To that end, we utilized VDT and peritumoral and intratumoral radiomic features to identify high-risk screen-detected lung cancers associated with poor survival outcomes. Among patients diagnosed with lung cancer at the first screening interval (T1), very-high risk patients had ex-
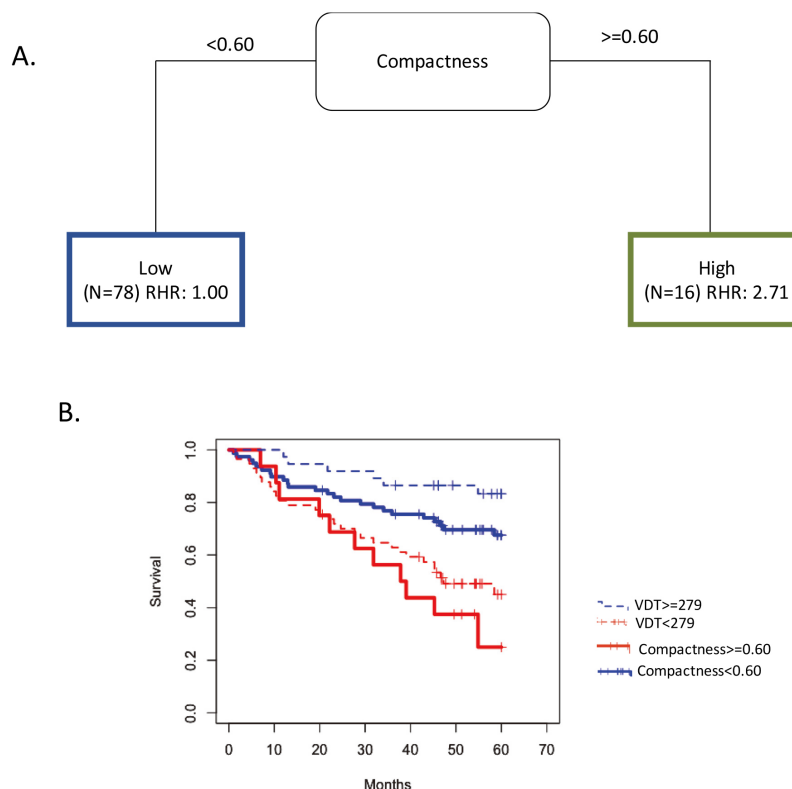
Fig. 4. Intratumoral feature Compactness and VDT have similar prognosis capabilities. (A) The tree structure of the classification and regression tree analysis (CART) which identified the survival cutpoint of compactness. (B) Overall Survival for VDT dichotomized at 279 days and Compactness dichotomized at 0.60. Abbreviations: RHR = relative hazard ratio.
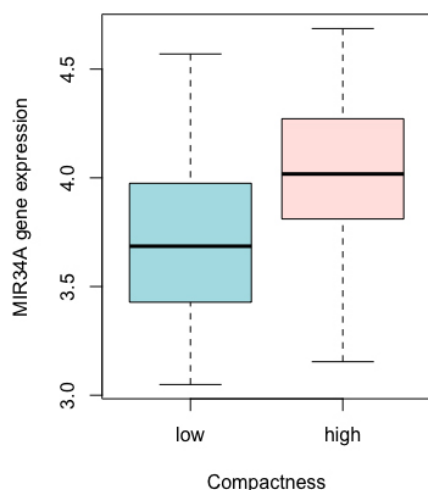

Fig. 5. Association between radiomics and gene expression. *MIR34A* expression by dichotomizing Compactness at the median.

tremely poor survival outcomes (HR = 11.71; 21.4% 5-year OS) versus the low-risk group (HR = 1.00; 82.1% 5-year OS). Among early-stage patients, the very-high risk group had extremely poor survival outcomes (HR = 11.71; 21.4% 5-year OS) versus the low-risk group (HR = 1.00; 82.1% 5-year OS). When combined patients diagnosed with lung cancer at the first (T1) and second (T2) screening intervals, patients in the high-risk group also exhibited extremely poor survival outcomes (HR = 8.15; 25% 5-year OS) versus the low-risk group (HR = 1.00; 83.3% 5-year OS; C-index = 0.69). Among early-stage patients, the high-risk patients had poor survival outcomes (HR = 9.07; 44.4% 5-year OS) versus the low-risk group (HR = 1.00; 90.9% 5-year OS).

VDT has been largely utilized as a diagnostic biomarker to discriminate malignant and benign nodules [8,31,53]; however, the thresholds to discriminate between malignant and benign pulmonary nodules are inconsistent. Additionally, prior studies utilized VDT as a biomarker to differentiate between indolent and aggressive lung cancers diagnosed [5,21,36,50,51] and have also utilized VDT as a prognostic factor [32,40,49]. For example, a VDT of less than 400 days was found to be an independent risk factor for poor disease-free survival [32]. In a study based on chest x-rays, the 5-year survival rate of fast-growing

nodules with a VDT of < 113 days was associated with significantly lower than slow-growing nodules with a VDT > 113 days [49]. Setojima et al. separated whole tumor VDT (WVDT) and solid-part tumor VDT (SVDT) and identified cut-offs 214 days for WVDT and less than 215 days for SVDT that were associated with poor recurrence-free survival and overall survival [40]. The decision tree in our analysis identified novel VDT thresholds (VDTs of 234 and 279) that exhibited independent capacity to discriminate between high-risk/aggressive tumors and low-risk/indolent tumors. Because a VDT between 20 and 400 days represents a high likelihood of malignancy, the cumulative evidence suggests that this broad range is capturing heterogeneous behaviors, including lower risk cancers such as indolent and slowing growing tumors.

While prior studies by group have utilized radiomic features only [37] and the combination of radiomics and an *a priori* VDT threshold [29] (i.e., < 400 vs. ⩾ 400) as predictors of lung cancer behavior, this is the first study to identify novel VDT thresholds in combination of radiomics to characterize the lethal potential of lung cancers diagnosed in lung cancer screening. Another novel aspect of this work is that we identified a single timepoint, baseline radiomic feature (compactness) that predicts VDT and identified potential biological underpinnings of VDT (Fig. 4). Because VDT is a delta-radiomic that requires serial images over time to calculate, a radiomic feature from a single timepoint that could act as a surrogate could be important because VDT could be calculated through a proxy. Interestingly, the compactness radiomic feature had similar prognostic capabilities as VDT (Fig. 4B). Compactness is a measure of how compact the shape of the tumor is relative to a sphere and, much like VDT, has been found to be a diagnostic feature that differentiates malignant from benign nodules [22,26]. Prior work has also show that compactness is associated with survival [3]. Additionally, our radiogenomics analyses revealed that high compactness is associated with a high expression of the *MIR34A* gene. MicroRNA 34a (miR-34a) is a microRNA that is encoded by the *MIR34A* gene and the miR-34 family members are tumor suppressive miRNAs appear to have a crucial role in repressing tumor progression by involving in epithelial-mesenchymal transition (EMT) via EMT-transcription factors, p53, and other signally pathways [19,20,54]. In prior studies, high expression of MIR34A in plasma and tumor tissue was associated with prolonged overall survival and disease-free survival among non-small cell lung cancer patients [55]. Interestingly, Aherne et al.

found that MIR34A was significantly increased in the adenoma and early-stage cancer groups compared to controls [4]. However, the role of *MIR34A* on nodule growth and behavior is currently unknown.

We acknowledge some limitations of this study. First, the sample size is modest because we utilized lung cancer cases with specific inclusion and exclusion criteria from the NLST. However, we utilized bootstrapping for internal validation which revealed the models were well calibrated. Hopefully other lung cancer screening trials, such as NELSON [11], LUSI [6], and MILD [33], will make their images and data public so that independent validation analyses can be performed. Additional research is also needed to validate the biological underpinnings of the gene identified in the radiogenomics analysis.

The results from our analyses revealed that radiomics combined with VDT can identify a vulnerable subset of screen-detected lung cancers that are associated with poor survival outcome suggesting such patients may need more aggressive treatment, such as adjuvant therapies, and more aggressive surveillance/follow-up. Further research is needed to validate these findings in other lung cancer screening trials and programs and to fully elucidate the biological underpinnings of these radiomic features and VDT.

Acknowledgments

Author contributions

Conception: J.P-M, R.J.G, M.B.S
Interpretation or analysis of data: J.P-M, H.L, W.M, I.T,T.K, S.A.E, M.B.S
Preparation of the manuscript: J.P-M, H.L, W.M, I.T, T.K, S.A.E, Y.B, R.J.G, M.B.S
Revision for important intellectual content: J.P-M, H.L, W.M, I.T, T.K, S.A.E, Y.B, R.J.G, M.B.S
Supervision: M.B.S and R.J.G

Conflict of interest

R.J.G is a consultant for *HealthMyne* Imaging Systems. J.P-M, H.L, W.M, I.T, T.K, S.A.E, Y.B, R.J.G, and M.B.S. declare no competing interests.

Supplementary data

The supplementary files are available to download from http://dx.doi.org/10.3233/CBM-210194.

References

[1] D.R. Aberle, A.M. Adams, C.D. Berg, W.C. Black, J.D. Clapp, R.M. Fagerstrom, I.F. Gareen, C. Gatsonis, P.M. Marcus and J.D. Sicks, Reduced lung-cancer mortality with low-dose computed tomographic screening, *N Engl J Med* **365** (2011), 395–409.

[2] D.R. Aberle, C.D. Berg, W.C. Black, T.R. Church, R.M. Fagerstrom, B. Galen, I.F. Gareen, C. Gatsonis, J. Goldin, J.K. Gohagan, B. Hillman, C. Jaffe, B.S. Kramer, D. Lynch, P.M. Marcus, M. Schnall, D.C. Sullivan, D. Sullivan and C.J. Zylak, The National Lung Screening Trial: Overview and study design, *Radiology* **258** (2011), 243–253.

[3] H.J.W.L. Aerts, E.R. Velazquez, R.T.H. Leijenaar, C. Parmar, P. Grossmann, S. Carvalho, J. Bussink, R. Monshouwer, B. Haibe-Kains, D. Rietveld, F. Hoebers, M.M. Rietbergen, C.R. Leemans, A. Dekker, J. Quackenbush, R.J. Gillies and P. Lambin, Decoding tumour phenotype by noninvasive imaging using a quantitative radiomics approach, *Nature Communications* **5** (2014), 4006.

[4] S.T. Aherne, S.F. Madden, D.J. Hughes, B. Pardini, A. Naccarati, M. Levy, P. Vodicka, P. Neary, P. Dowling and M. Clynes, Circulating miRNAs miR-34a and miR-150 associated with colorectal cancer progression, *BMC Cancer* **15** (2015), 329.

[5] D.R. Baldwin, S.W. Duffy, N.J. Wald, R. Page, D.M. Hansell and J.K. Field, UK Lung Screen (UKLS) nodule management protocol: Modelling of a single screen randomised controlled trial of low-dose CT screening for lung cancer, *Thorax* **66** (2011), 308–313.

[6] N. Becker, E. Motsch, A. Trotter, C.P. Heussel, H. Dienemann, P.A. Schnabel, H.U. Kauczor, S.G. Maldonado, A.B. Miller, R. Kaaks and S. Delorme, Lung cancer mortality reduction by LDCT screening-Results from the randomized German LUSI trial, *Int J Cancer* **146** (2020), 1503–1513.

[7] J. Brodersen, T. Voss, F. Martiny, V. Siersma, A. Barratt and B. Heleno, Overdiagnosis of lung cancer with low-dose computed tomography screening: Meta-analysis of the randomised clinical trials, *Breathe (Sheff)* **16** (2020), 200013.

[8] M.E. Callister, D.R. Baldwin, A.R. Akram, S. Barnard, P. Cane, J. Draffan, K. Franks, F. Gleeson, R. Graham, P. Malhotra, M. Prokop, K. Rodger, M. Subesinghe, D. Waller and I. Woolhouse, British Thoracic Society guidelines for the investigation and management of pulmonary nodules, *Thorax* **70**(Suppl 2) (2015), ii1–ii54.

[9] D. Cherezov, S.H. Hawkins, D.B. Goldgof, L.O. Hall, Y. Liu, Q. Li, Y. Balagurunathan, R.J. Gillies and M.B. Schabath, Delta radiomic features improve prediction for lung cancer

[10] incidence: A nested case-control analysis of the National Lung Screening Trial, *Cancer Med* **7** (2018), 6340–6356.

[10] R. Clay, S. Rajagopalan, R. Karwoski, F. Maldonado, T. Peikert and B. Bartholmai, Computer Aided Nodule Analysis and Risk Yield (CANARY) characterization of adenocarcinoma: radiologic biopsy, risk stratification and future directions, *Transl Lung Cancer Res* **7** (2018), 313–326.

[11] H.J. de Koning, C.M. van der Aalst, P.A. de Jong, E.T. Scholten, K. Nackaerts, M.A. Heuvelmans, J.-W.J. Lammers, C. Weenink, U. Yousaf-Khan and N.J.N.E.j.o.m. Horeweg, Reduced lung-cancer mortality with volume CT screening in a randomized trial, **382** (2020), 503–513.

[12] B. Dreno, J.F. Thompson, B.M. Smithers, M. Santinami, T. Jouary, R. Gutzmer, E. Levchenko, P. Rutkowski, J.J. Grob, S. Korovin, K. Drucis, F. Grange, L. Machet, P. Hersey, I. Krajsova, A. Testori, R. Conry, B. Guillot, W.H.J. Kruit, L. Demidov, J.A. Thompson, I. Bondarenko, J. Jaroszek, S. Puig, G. Cinat, A. Hauschild, J.J. Goeman, H.C. van Houwelingen, F. Ulloa-Montoya, A. Callegaro, B. Dizier, B. Spiessens, M. Debois, V.G. Brichard, J. Louahed, P. Therasse, C. Debruyne and J.M. Kirkwood, MAGE-A3 immunotherapeutic as adjuvant therapy for patients with resected, MAGE-A3-positive, stage III melanoma (DERMA): A double-blind, randomised, placebo-controlled, phase 3 trial, *Lancet Oncol* **19** (2018), 916–929.

[13] X. Fave, L. Zhang, J. Yang, D. Mackin, P. Balter, D. Gomez, D. Followill, A.K. Jones, F. Stingo, Z. Liao, R. Mohan and L. Court, Delta-radiomics features for the prediction of patient outcomes in non-small cell lung cancer, *Sci Rep* **7** (2017), 588.

[14] D.S. Gierada, P. Pinsky, H. Nath, C. Chiles, F. Duan and D.R. Aberle, Projected outcomes using different nodule sizes to define a positive CT lung cancer screening examination, *J Natl Cancer Inst* **106** (2014).

[15] R.J. Gillies and M.B. Schabath, Radiomics improves cancer screening and early detection, *Cancer Epidemiol Biomarkers Prev* **29** (2020), 2556–2567.

[16] F. Harrell, Regression Modeling Strategies version 6.1-1, 2021.

[17] S. Hawkins, H. Wang, Y. Liu, A. Garcia, O. Stringfield, H. Krewer, Q. Li, D. Cherezov, R.A. Gatenby, Y. Balagurunathan, D. Goldof, M.B. Schabath, L. Hall and R.J. Gillies, Predicting Malignant Nodules from Screening CT Scans, *J Thorac Oncol* **11** (2016), 2120–2128.

[18] B. Heleno, V. Siersma and J. Brodersen, Estimation of overdiagnosis of lung cancer in low-dose computed tomography screening: A secondary analysis of the danish lung cancer screening trial, *JAMA Intern Med* **178** (2018), 1420–1422.

[19] H. Hermeking, The miR-34 family in cancer and apoptosis, *Cell Death & Differentiation* **17** (2010), 193–199.

[20] H. Hermeking, MicroRNAs in the p53 network: micromanagement of tumour suppression, *Nat Rev Cancer* **12** (2012), 613–626.

[21] M.A. Heuvelmans, M. Oudkerk, G.H. de Bock, H.J. de Koning, X. Xie, P.M. van Ooijen, M.J. Greuter, P.A. de Jong, H.J. Groen and R. Vliegenthart, Optimisation of volume-doubling time cutoff for fast-growing lung nodules in CT lung cancer screening reduces false-positive referrals, *Eur Radiol* **23** (2013), 1836–1845.

[22] W. Jun, L. Xia, D. Di, S. Jiangdian, X. Min, Z. Yali and T. Jie, Prediction of malignant and benign of lung tumor using a quantitative radiomic method, *Annu Int Conf IEEE Eng Med Biol Soc* **2016** (2016), 1272–1275.

[23] M. Kanashiki, T. Tomizawa, I. Yamaguchi, K. Kurishima, N. Hizawa, H. Ishikawa, K. Kagohashi and H. Satoh, Volume doubling time of lung cancers detected in a chest radiograph mass

screening program: Comparison with CT screening, *Oncol Lett* **4** (2012), 513–516.

[24] J.P. Ko, E.J. Berman, M. Kaur, J.S. Babb, E. Bomsztyk, A.K. Greenberg, D.P. Naidich and H. Rusinek, Pulmonary Nodules: Growth rate assessment in patients by using serial CT and three-dimensional volumetry, *Radiology* **262** (2012), 662–671.

[25] P. Lambin, E. Rios-Velazquez, R. Leijenaar, S. Carvalho, R.G. van Stiphout, P. Granton, C.M. Zegers, R. Gillies, R. Boellard, A. Dekker and H.J. Aerts, Radiomics: Extracting more information from medical images using advanced feature analysis, *Eur J Cancer* **48** (2012), 441–446.

[26] E.J. Limkin, S. Reuzé, A. Carré, R. Sun, A. Schernberg, A. Alexis, E. Deutsch, C. Ferté and C. Robert, The complexity of tumor shape, spiculatedness, correlates with tumor radiomic shape features, *Scientific Reports* **9** (2019), 4329.

[27] R.M. Lindell, T.E. Hartman, S.J. Swensen, J.R. Jett, D.E. Midthun, H.D. Tazelaar and J.N. Mandrekar, Five-year lung cancer screening experience: CT appearance, growth rate, location, and histologic features of 61 lung cancers, *Radiology* **242** (2007), 555–562.

[28] Y. Liu, H. Wang, Q. Li, M.J. McGettigan, Y. Balagurunathan, A.L. Garcia, Z.J. Thompson, J.J. Heine, Z. Ye, R.J. Gillies and M.B. Schabath, Radiologic features of small pulmonary nodules and lung cancer risk in the national lung screening trial: A nested case-control study, *Radiology* **286** (2017), 298–306.

[29] H. Lu, W. Mu, Y. Balagurunathan, J. Qi, M.A. Abdalah, A.L. Garcia, Z. Ye, R.J. Gillies and M.B. Schabath, Multi-window CT based Radiomic signatures in differentiating indolent versus aggressive lung cancers in the National Lung Screening Trial: A retrospective study, *Cancer Imaging* **19** (2019), 45.

[30] P. Maisonneuve, V. Bagnardi, M. Bellomi, L. Spaggiari, G. Pelosi, C. Rampinelli, R. Bertolotti, N. Rotmensz, J.K. Field, A. Decensi and G. Veronesi, Lung cancer risk prediction to select smokers for screening CT – a model based on the Italian COSMOS trial, *Cancer Prev Res (Phila)* **4** (2011), 1778–1789.

[31] A. Nair, A. Devaraj, M.E.J. Callister and D.R. Baldwin, The Fleischner Society 2017 and British Thoracic Society 2015 guidelines for managing pulmonary nodules: Keep calm and carry on, *Thorax* **73** (2018), 806.

[32] S. Park, S.M. Lee, S. Kim, J.G. Lee, S. Choi, K.H. Do and J.B. Seo, Volume doubling times of lung adenocarcinomas: Correlation with predominant histologic subtypes and prognosis, *Radiology* **295** (2020), 703–712.

[33] U. Pastorino, M. Silva, S. Sestini, F. Sabia, M. Boeri, A. Cantarutti, N. Sverzellati, G. Sozzi, G. Corrao and A. MarchianòijŇ Prolonged lung cancer screening reduced 10-year mortality in the MILD trial: New confirmation of lung cancer screening efficacy, *Ann Oncol* **30** (2019), 1162–1169.

[34] E.F. Patz, Jr, P. Pinsky and B.S. Kramer, Estimating Overdiagnosis in Lung Cancer Screening – ReplyLetters, *JAMA Internal Medicine* **174** (2014), 1198–1199.

[35] E.F. Patz, Jr, P. Pinsky, C. Gatsonis, J.D. Sicks, B.S. Kramer, M.C. Tammemägi, C. Chiles, W.C. Black and D.R. Aberle, Overdiagnosis in low-dose computed tomography screening for lung cancer, *JAMA Intern Med* **174** (2014), 269–274.

[36] J.H. Pedersen, H. Ashraf, A. Dirksen, K. Bach, H. Hansen, P. Toennesen, H. Thorsen, J. Brodersen, B.G. Skov, M. Døssing, J. Mortensen, K. Richter, P. Clementsen and N. Seersholm, The Danish randomized lung cancer CT screening trial-overall design and results of the prevalence round, *J Thorac Oncol* **4** (2009), 608–614.

[37] J. Pérez-Morales, I. Tunali, O. Stringfield, S.A. Eschrich, Y. Balagurunathan, R.J. Gillies and M.B. Schabath, Peritumoral

and intratumoral radiomic features predict survival outcomes among patients diagnosed in lung cancer screening, *Sci Rep* **10** (2020), 10528.

[38] M.B. Schabath, P.P. Massion, Z.J. Thompson, S.A. Eschrich, Y. Balagurunathan, D. Goldof, D.R. Aberle and R.J. Gillies, Differences in Patient Outcomes of Prevalence, Interval, and Screen-Detected Lung Cancers in the CT Arm of the National Lung Screening Trial, *PLoS One* **11** (2016), e0159880.

[39] M.B. Schabath, E.A. Welsh, W.J. Fulp, L. Chen, J.K. Teer, Z.J. Thompson, B.E. Engel, M. Xie, A.E. Berglund, B.C. Creelan, S.J. Antonia, J.E. Gray, S.A. Eschrich, D.T. Chen, W.D. Cress, E.B. Haura and A.A. Beg, Differential association of STK11 and TP53 with KRAS mutation-associated gene expression, proliferation and immune surveillance in lung adenocarcinoma, *Oncogene* **35** (2016), 3209–3216.

[40] Y. Setojima, Y. Shimada, T. Tanaka, S. Shigefuku, Y. Makino, S. Maehara, M. Hagiwara, R. Masuno, T. Yamada, M. Kakihana, N. Kajiwara, T. Ohira, and N. Ikeda, Prognostic impact of solid-part tumour volume doubling time in patients with radiological part-solid or solid lung cancer, *Eur J Cardiothorac Surg* **57** (2020), 763–770.

[41] S. Sone, T. Nakayama, T. Honda, K. Tsushima, F. Li, M. Haniuda, Y. Takahashi, T. Suzuki, T. Yamanda, R. Kondo, T. Hanaoka, F. Takayama, K. Kubo and H. Fushimi, Long-term follow-up study of a population-based 1996–1998 mass screening programme for lung cancer using mobile low-dose spiral computed tomography, *Lung Cancer* **58** (2007), 329–341.

[42] S. Srivastava, E.J. Koay, A.D. Borowsky, A.M. De Marzo, S. Ghosh, P.D. Wagner and B.S. Kramer, Cancer overdiagnosis: A biological challenge and clinical dilemma, *Nat Rev Cancer* **19** (2019), 349–358.

[43] K. Ten Haaf and H.J. de Koning, Overdiagnosis in lung cancer screening: Why modelling is essential, *J Epidemiol Community Health* **69** (2015), 1035–1039.

[44] K. Ten Haaf, J. Jeon, M.C. Tammemägi, S.S. Han, C.Y. Kong, S.K. Plevritis, E.J. Feuer, H.J. de Koning, E.W. Steyerberg and R. Meza, Risk prediction models for selection of lung cancer screening candidates: A retrospective validation study, *PLoS Med* **14** (2017), e1002277.

[45] R. Thawani, M. McLane, N. Beig, S. Ghose, P. Prasanna, V. Velcheti and A. Madabhushi, Radiomics and radiogenomics in lung cancer: A review for the clinician, *Lung Cancer* **115** (2018), 34–41.

[46] M. Treskova, I. Aumann, H. Golpon, J. Vogel-Claussen, T. Welte and A. Kuhlmann, Trade-off between benefits, harms and economic efficiency of low-dose CT lung cancer screening: A microsimulation analysis of nodule management strategies in a population-based setting, *BMC medicine* **15** (2017), 162–162.

[47] I. Tunali, R.J. Gillies and M.B. Schabath, Application of radiomics and artificial intelligence for lung cancer precision medicine, *Cold Spring Harb Perspect Med* (2021).

[48] I. Tunali, L.O. Hall, S. Napel, D. Cherezov, A. Guvenis, R.J. Gillies and M.B. Schabath, Stability and reproducibility of computed tomography radiomic features extracted from peritumoral regions of lung cancer lesions, *Med Phys* **46** (2019), 5075–5085.

[49] K. Usuda, Y. Saito, M. Sagawa, M. Sato, K. Kanma, S. Takahashi, C. Endo, Y. Chen, A. Sakurada and S. Fujimura, Tumor doubling time and prognostic assessment of patients with primary lung cancer, *Cancer* **74** (1994), 2239–2244.

[50] R.J. van Klaveren, M. Oudkerk, M. Prokop, E.T. Scholten, K. Nackaerts, R. Vernhout, C.A. van Iersel, K.A. van den Bergh,

S. van 't Westeinde, C. van der Aalst, E. Thunnissen, D.M. Xu, Y. Wang, Y. Zhao, H.A. Gietema, B.J. de Hoop, H.J. Groen, G.H. de Bock, P. van Ooijen, C. Weenink, J. Verschakelen, J.W. Lammers, W. Timens, D. Willebrand, A. Vink, W. Mali and H.J. de Koning, Management of lung nodules detected by volume CT scanning, *N Engl J Med* **361** (2009), 2221–2229.

[51] G. Veronesi, P. Maisonneuve, M. Bellomi, C. Rampinelli, I. Durli, R. Bertolotti and L. Spaggiari, Estimating overdiagnosis in low-dose computed tomography screening for lung cancer: A cohort study, *Ann Intern Med* **157** (2012), 776–784.

[52] H.G. Welch and W.C. Black, Overdiagnosis in cancer, *J Natl Cancer Inst* **102** (2010), 605–613.

[53] D.F. Yankelevitz and C.I. Henschke, Does 2-year stability imply that pulmonary nodules are benign? *AJR Am J Roentgenol* **168** (1997), 325–328.

[54] L. Zhang, Y. Liao and L. Tang, MicroRNA-34 family: A potential tumor suppressor and therapeutic candidate in cancer, *J Exp Clin Cancer Res* **38** (2019), 53.

[55] K. Zhao, J. Cheng, B. Chen, Q. Liu, D. Xu and Y. Zhang, Circulating microRNA-34 family low expression correlates with poor prognosis in patients with non-small cell lung cancer, *Journal of Thoracic Disease* **9** (2017), 3735–3746.

[56] A. Zwanenburg, M. Vallières, M.A. Abdalah, H.J.W.L. Aerts, V. Andrearczyk, A. Apte, S. Ashrafinia, S. Bakas, R.J. Beukinga, R. Boellaard, M. Bogowicz, L. Boldrini, I. Buvat, G.J.R. Cook, C. Davatzikos, A. Depeursinge, M.-C. Desseroit, N. Dinapoli, C.V. Dinh, S. Echegaray, I. El Naqa, A.Y. Fedorov, R. Gatta, R.J. Gillies, V. Goh, M. Götz, M. Guckenberger, S.M. Ha, M. Hatt, F. Isensee, P. Lambin, S. Leger, R.T.H. Leijenaar, J. Lenkowicz, F. Lippert, A. Losnegård, K.H. Maier-Hein, O. Morin, H. Müller, S. Napel, C. Nioche, F. Orlhac, S. Pati, E.A.G. Pfaehler, A. Rahmim, A.U.K. Rao, J. Scherer, M.M. Siddique, N.M. Sijtsema, J. Socarras Fernandez, E. Spezi, R.J.H.M. Steenbakkers, S. Tanadini-Lang, D. Thorwarth, E.G.C. Troost, T. Upadhaya, V. Valentini, L.V. van Dijk, J. van Griethuysen, F.H.P. van Velden, P. Whybra, C. Richter and S. Löck, The image biomarker standardization initiative: Standardized quantitative radiomics for high-throughput image-based phenotyping, *Radiology* **295** (2020), 328–338.